

Observations of Internal Rotor Structure using an Instrumented Sailplane

Rolf F. Hertenstein
CoRA Division of Northwest Research Associates
Boulder, Colorado 80302 USA
herten@cora.nwra.com

and

Charles L. Martin
National Center for Atmospheric Research
Boulder, Colorado 80301 USA
martinc@ucar.edu

Abstract

We present preliminary results from an observational study using an instrumented sailplane along the Front Range of the Colorado Rocky Mountains. Our goal is to measure the internal structure of rotors associated with mountain lee waves. From 24 penetrations of rotors on four different days we were able to identify primary up-and-down branches within the rotor. Numerous small-scale turbulent eddies within the parent rotor were analyzed as well. Future research possibilities based on these encouraging preliminary results are discussed.

Introduction

Soaring pilots have dealt with rotors since the early discovery of lee waves.^{1, 2} Rotor turbulence can be mild, is most often moderate to severe, and in a few (fortunately rare) cases, extreme. In this paper, the term rotor will be used in the sense most common to soaring pilots; that is, rotors are the turbulent regions below laminar wave flow.

Based on the experience of soaring pilots, we know rotors sometimes have quasi-organized branches. Turbulent updrafts are found on the rotor leading (upwind) side adjacent to the laminar wave updraft, while turbulent downdrafts are found on the downwind side of the rotor. At other times, there is no recognizable organization within the turbulent rotor.

Another well-known feature of lee waves and rotors is their distinctive interface, which takes the pilot from unpleasant turbulence to incredibly smooth wave flow, often within a few seconds.

Modeling studies have shed some light on the possible internal structure of rotors.³ Rotors identified as Type-1 are associated with resonant (also called trapped) waves, have a quasi-organized internal circulation, and are those most commonly illustrated in references to mountain lee waves. Rotors identified as Type-2 resemble a hydraulic jump and are less common, with a completely different structure compared to Type-1 rotors. Figure 1 shows examples of two rotor types that were simulated using a high-resolution numerical model. No unambiguous direct measurements of a Type-2 rotor are known.

Regardless of whether or not quasi-organized branches exist, soaring pilots know that rotors also consist of many embedded small-scale turbulent gusts. Numerical models have also begun to explore these smaller-scale structures within the rotor, referred to as sub-rotors⁴. Sub-rotors appear to form

along the leading edge of the parent rotor, then subsequently propagate and mix within the rotor, in agreement with observations that rotors are usually most turbulent along the leading edge.⁵

A research effort has begun along the Rocky Mountain Front Range near Boulder, Colorado, using an instrumented sailplane. The goals of the research include documenting rotor structure and the wave/rotor interface, as well as investigating the size and intensity of sub-rotors. We are especially interested in confirming the existence of Type-2 rotors.

In the following sections we discuss the research effort and preliminary results from flights during the winter of 2006-2007.

Observational platform and technique

In this section we describe the observational platform, flight paths used to sample the rotor, and present a summary of the case study days.

The sailplane and instrumentation

The instrumented sailplane, a two-place Schweizer 2-32, is the former "Explorer" used by the National Center for Atmospheric Research (NCAR). The sturdy Explorer is ideal for the research effort, allowing low-cost, efficient, and high-resolution sampling of the rotor.

Two primary instruments are installed in the Explorer for data collection. The first is a Cambridge 302 Direct Digital Variometer (DDV), originally designed for sport soaring. The DDV system features barometric (static) and dynamic pressure sensors as well as a total energy probe. Since the sink rate at various indicated airspeeds is known from the sailplane's polar curve, the vertical velocity of the air can be easily derived.

The DDV also includes an onboard Global Positioning System (GPS), which is driven by a Garmin GPS-25. All data from the DDV is recorded at a frequency of 1 Hz.

The second instrument is a MicroStrain 3DM-G Gyro Enhanced Orientation Sensor, which measures the three degrees of its orientation relative to the earth. The 3DM-G records three-dimensional accelerations, heading, and rate gyroscope. Combined with DDV and GPS data, horizontal winds can be calculated. In addition, the accelerometer records turbulence in multiples of 'g', i.e., multiples of the earth's gravity. At the time of this writing, there are still calibration issues with the 3DM-G, thus we will be discussing only results derived from the DDV.

The two instruments provided serial data feeds to an onboard low-power embedded computer system. The Linux-based computer saved formatted data files on solid state media, and the files were retrieved after each flight.

Data collection flights can be accomplished inexpensively and efficiently with this system. Typically two to four hours of data were collected on any one flight.

Although the Explorer has many advantages, there are, of course, limitations to using a sailplane for atmospheric measurements. First, being a sailplane, the Explorer depends on updrafts for prolonged data-collection flights. Second, the sailplane has a limited payload compared to powered research aircraft, which necessitates the relatively simple instrument package. Third, the Explorer may be flown only under Visual Flight Rules, i.e., no sampling in cloud is possible. The benefits of low cost and simplicity far outweigh the limitations.

Selection of case-study days for data-collection flights

Mountain waves and rotors frequently occur along the Front Range during fall, winter, and spring. Standard forecast products freely available on the internet, e.g., model forecasts of winds aloft, provided two to three days warning of potential data collection days.

The Indian Peaks area of the Front Range west of Boulder features topography that is quasi-two-dimensional. Observation of lenticular and/or rotor clouds, as well as flight experience, indicates that the wave response is also quasi-two-dimensional when the flow is within about 10 degrees of westerly, or perpendicular to the north-south orientation of the Indian Peaks. Deviations from two-dimensionality are known to exist due to details of the topography, e.g., gaps in the higher terrain. The flights described here concentrated on days with little deviation from westerly flow. Unfortunately, during the winter of 2006-2007 two major snowstorms within a short period closed operations completely for about six weeks, limiting the number of research flights.

Typical flight track for sampling the rotor

Our primary flight strategy for sampling both the internal rotor structure and the wave-rotor interface was simple. Once

established in the wave, we identified the height of the rotor top (if not obvious from rotor clouds). We then flew repeated circuits (see sample flight track in Fig. 1a). Each comprised a climb in wave lift (using short north-south aligned crosswind legs), a downwind (eastward) leg over the rotor, a short leg in the wave sink, followed by an upwind (westward) leg directly through the rotor. The rotor sampling strategy was efficient, and allowed for several rotor penetrations in a relatively short time. All research flights took place between late morning and mid afternoon local time.

Summary of case study days

Figure 2 shows terrain and approximate locations of successful rotor penetrations. Table 1 summarizes seven days during the wave season 2006-2007 on which data collection was attempted. Of these, four case days supplied useful recorded data from a total of 24 successful rotor penetrations. Two entries are found for 21 November 2006. Eight penetrations were flown in one location while the other four were flown about 5 km further south along the primary wave. On 8 November 2006 conditions were completely dry (no wave or rotor clouds) but well-defined secondary and primary harmonics were present. Only the primary rotor was sampled. On 13 November 2006, a deep foehn wall with an indistinct top was present over the mountains. During the day it deepened, with clouds and showers drifting almost 20 km from the mountain crest. Waves and rotors were non-stationary and short-lived, making sampling of the rotor challenging. Rotor clouds were also not present during research flights on 21 November 2006 and 05 March 2007.

Three flights that did not result in collection of useful data are indicated by the zeros (0) in Table 1. On 17 November 2006, rotor clouds were deep with relatively low bases, and rotor penetrations in free flight were not feasible (although wave lift provided a climb to 7500 m). On 19 February 2007, the air mass rapidly lost stability, leading to deep cumulus but no organized wave or rotor. Finally, on 21 February 2007, 12 rotor penetrations were flown, however, the 1 Hz data collection failed (the reason has since been identified and remedied). Attempts to reconstruct the rotor penetrations from the 4-second data within the recorded IGC file were not successful.

We had hoped that useful measurements of the rotor could also be obtained during the aero-tow. But for reasons that are not clear, the data during the entire aero-tow is too noisy, and aero-tow through the rotor is not distinguishable from the rest of the aero-tow.

Results

We now discuss results from the four research flights during which rotor penetrations were flown and data successfully recorded. Figure 3 shows vertical velocity for three of the six rotor penetrations flown on 8 November 2006.

Vertical velocity is derived from the Cambridge 302 DDV data recorded at 1 Hz. The raw variometer data are adjusted for the sailplane sink rate, based on the altitude-corrected airspeed and sailplane polar. An approximate sailplane heading during various parts of the sampling is indicated above the time series. Thus, Fig. 3 is not showing a series of rotors downwind of a barrier; rather it shows successive penetrations of one quasi-stationary rotor. Each phase of the flight (i.e., smooth wave updraft, smooth wave downdraft, and transition in and out of the turbulent rotor) is evident from the vertical velocity time series. Details of the vertical velocity distribution vary with each rotor penetration. For instance, in the first penetration (Fig. 3), the vertical gusts with the strongest speeds appear near the downwind side of the rotor. In the third penetration, the strongest vertical gust is near the upwind rotor side. Thus, the internal structure of the rotor appears to be rapidly evolving. This may be evidence for the existence of sub-rotors that have been simulated by numerical models⁴.

Evidence for quasi-organized circulations

Figure 4 shows the time series expanded for one rotor penetration flown on 8 November 2006. An upward trend in the vertical velocity is also qualitatively apparent from the time series through the rotor, as noted in most, if not all, the sampled rotors on each of the four data recording flights. This indicates that there is on average an upward branch along the upwind side of the rotor, and a downward branch on the downwind side of the rotor. As mentioned, the quasi-organized up-and-down branches within the rotor are well known to soaring pilots, but owing to a lack of fine-scale, direct measurements, their existence has been in doubt by some in the atmospheric science community.

A scatter plot is shown in Fig. 5 to summarize the six rotor penetrations flown on 8 November 2006. The total elapsed time for six rotor penetrations was approximately 2100 seconds (35 minutes). Each point plotted is one vertical velocity measurement at a specific longitude. The downwind side of the rotors is toward the left, while the upwind side is to the right. The slanted line is a linear fit of the data, from which the upward trend across the rotor is once again clear. And, as also indicated by Figs. 3 and 4, a great deal of small-scale variation in the vertical velocity distribution (leading to the characteristic sharp, rapidly evolving turbulence) is noted across the rotors.

Figure 6 shows a trace of height vs. longitude for each of the six rotor penetrations on 8 November 2006. The traces once again show descending motion on the downwind portion of the rotor and rising motion along the upwind side. Based on entry and exit points for each trace, the horizontal dimension of the rotor varies with height as expected. The rotor is also seen to be quasi, and not absolutely, stationary. For instance, the two rotor penetrations starting near 4800 m are offset by approximately 1 km, indicating a shift in wavelength (circles in Fig. 6).

Upwind rotor penetrations on the remaining three days on which useful data were recorded (see Table 1) show similar results. The upward trend, from which we infer the overall rotor circulation, is present in all the rotor penetrations we flew (even on 13 November 2006, when the waves and rotors were not stationary over the ground).

Non-stationary rotors – 13 November 2006

As already mentioned, this day was characterized by rapidly changing conditions. From shadows on the ground, we estimated that the rotor clouds were moving downwind at about 15 m/s. On one climb after a rotor penetration, the GPS trace indicates that in order to remain in the wave updraft, our position shifted 2.1 km over 2.6 minutes, indicating that the wave was traveling downwind at a speed of 13.5 m/s. The conditions were distinctly different than the quasi-stationary wave and rotor encountered on the other three days.

Two downwind rotor penetrations

On two occasions, we departed the wave system by flying *downwind* through the rotor. This was possible on two days when wave updrafts were relatively weak, on the order of 2 m/s. The two penetrations reveal a downward trend (flying from the upwind to downwind side of the rotor) in vertical velocities. This supports our analysis of overall rotor up-and-down branches.

Small-scale gusts within the main rotor

Numerous small-scale gusts within the parent rotor were encountered with each penetration. The time between gusts (i.e., changes in sign or magnitude of vertical velocity) within the rotor was typically one or two seconds, and sometimes as long as four seconds. This agrees well with our perception from the flights. In addition, the time series of vertical gust from the 3DM-G also showed variations on the order of 1 Hz. (Though, as mentioned, calibration difficulties did not allow us to quantify the magnitude of recorded data from the 3DM-G.)

We performed two checks to determine the reliability of vertical velocity derived from the DDV. First, we differentiated both barometric and GPS altitudes. Second, vertical accelerations were calculated. Both were found to be in general agreement with the DDV-derived vertical velocity. The exception was found in a number of extreme vertical velocity measurements from the DDV, which we estimate to be too high by a factor of 2. The reasons for these anomalies are unclear at this time. Thus, in what follows, we do not present maximum and minimum values, and the vertical velocity statistics should be viewed as approximate rather than absolute.

Table 2 summarizes average vertical velocity and standard deviation for small-scale gusts in the rotor updraft and downdraft branches. On most days, the standard deviation is close to the average value for both updrafts and downdrafts. The second set of rotor penetrations on 21 November 2006

produced larger standard deviations than the first set. The variability of rotor turbulence along the wave system on a specific day, or in one location on different days, is an interesting topic that will require many more flights to resolve. We emphasize again that the rotors encountered on all days were quite mild, with only occasional moderate turbulence.

Attempts were made to quantify the horizontal scale of the small-scale turbulent eddies. Calculations using GPS fixes most often yielded values between 20 m and 50 m, with a few eddies around 100 m. Unfortunately, the accuracy of the GPS fixes is only 15 m, thus the potential error is large.

Figure 7 shows the distribution of gusts derived from temporal changes in vertical velocity. In most cases, the majority of gusts are within 0.4 g of unaccelerated flight (i.e., 1 g). We were surprised to see that on the three penetrations during which most points were sampled, negative gusts (0.8 g) occurred slightly more frequently than positive gusts (1.2 g). In the mild rotors sampled on these flights, few gusts exceeding 2.0 g, or less than 0 g, were noted, in agreement with our in-flight classification of the turbulence.

Concluding remarks

Systematic measurements of rotors were made using an instrumented sailplane along the Colorado Front Range of the Rocky Mountains during the 2006-2007 wave season. On three of the days, the rotors sampled were Type-1³ and quasi-stationary. On one case day (13 November 2006), the rotors appeared to form and drift downwind, with transient waves above. No Type-2 rotors were encountered. (The first author has previously encountered rotors along the Colorado Rocky Mountain Front Range that behaved as if they were Type-2).

For the three Type-1 rotors sampled, evidence of organized turbulent up-and-down branches was identified, with updrafts on the upwind rotor side and downdrafts on the downwind rotor side. The fact that rotors often contain organized turbulent branches has long been known to soaring pilots, but to our knowledge, it has never been carefully documented. The rotors associated with the transient waves show similar updraft and downdraft branches.

Calculations were performed to quantify characteristics of small-scale eddies, or sub-rotors, within the parent rotor. We are encouraged by our preliminary results and foresee the possibility of using our data collection to verify findings from numerical model simulations.

We hope to continue exploring the internal structure of rotors. Increasing our data set over time and over many cases will allow a rigorous statistical analysis of rotors and sub-rotors. On future flights we also hope to verify the existence of the Type-2 rotor. Other future plans include improving the sailplane instrumentation (e.g., adding temperature recording capability). Use of the Microstrain 3DM-G gyro will also allow analysis of the horizontal wind field within the rotor and

wave. In addition, we plan to investigate cases along the Front Range that are more three-dimensional in nature. These situations occur along the Front Range when winds aloft are northwesterly (southwesterly flow is generally unfavorable for wave formation in this area).

Finally, we are considering the possibility of expanding our efforts to use the instrumented sailplane for fine-resolution measurements of the air within and surrounding thermals.

Acknowledgements

This research was supported by the National Science Foundation under grant ATM-0541729. Dr. Joachim Kuettner was vital in making the former NCAR "Explorer" available. Mr. Michael Exner was responsible for installing the instrumentation. Soaring Society of Boulder pilots (especially Mr. Rod Smythe) are thanked for providing aero-tows.

References

- ¹Kuettner, J. P., "Moazagotl und Föhnwelle." *Beitr. Phys. Frei Atmos.*, 25, 1938, 79-114.
- ²Kuettner, J. P., "Zur Entstehung der Föhnwalle." *Beitr. Phys. Frei Atmos.*, 25, 1939, 251-299
- ³Hertenstein, R. F., and J. P. Kuettner, "Rotor types associated with steep lee topography: Influence of the wind profile." *Tellus*, 47, 2005, 310-326.
- ⁴Doyle, J. D., and D. R. Durran, "Rotor and sub-rotor dynamics in the lee of three dimensional terrain." *J. Atmos. Sci.*, 64, 2007, 4202-4221.
- ⁵Lester, P. F., and W. A. Fingerhut, "Lower turbulent zones associated with lee waves." *J. Appl. Meteorol.*, 13, 1974, 54-61.

Table 1
Summary of research flights.

Date	Cloud markers	Number of recorded rotor penetrations	Rotor turbulence
08 Nov 06	None	6	Mild, occasional moderate
13 Nov 06	Deep foehn, few rotor clouds	3	Moderate
17 Nov 06	Relatively deep rotor cloud	0	Mild
21 Nov 06 - a	High lenticular	8	Mild, occasional moderate
21 Nov 06 - b	High lenticular	4	Mild, occasional moderate
19 Feb 07	Cumulus congestus with pileus	0	Mild - convective
21 Feb 07	A few small rotor clouds	0	Mild to moderate
05 Mar 07	High lenticular	3	Mild

Table 2
Vertical velocity statistics for small-scale turbulent eddy updrafts and downdrafts

	08-Nov-06	13-Nov-06	21-Nov-06a	21-Nov-06b	05-Mar-07
Average updraft	3.1	2.9	1.9	2.7	2.9
Average downdraft	-2.5	-2.5	-1.8	-1.9	-3.2
Std. Deviation updraft	2.4	2.7	1.7	2.2	3.3
Std. Deviation downdraft	1.9	2.0	1.5	1.9	3.0

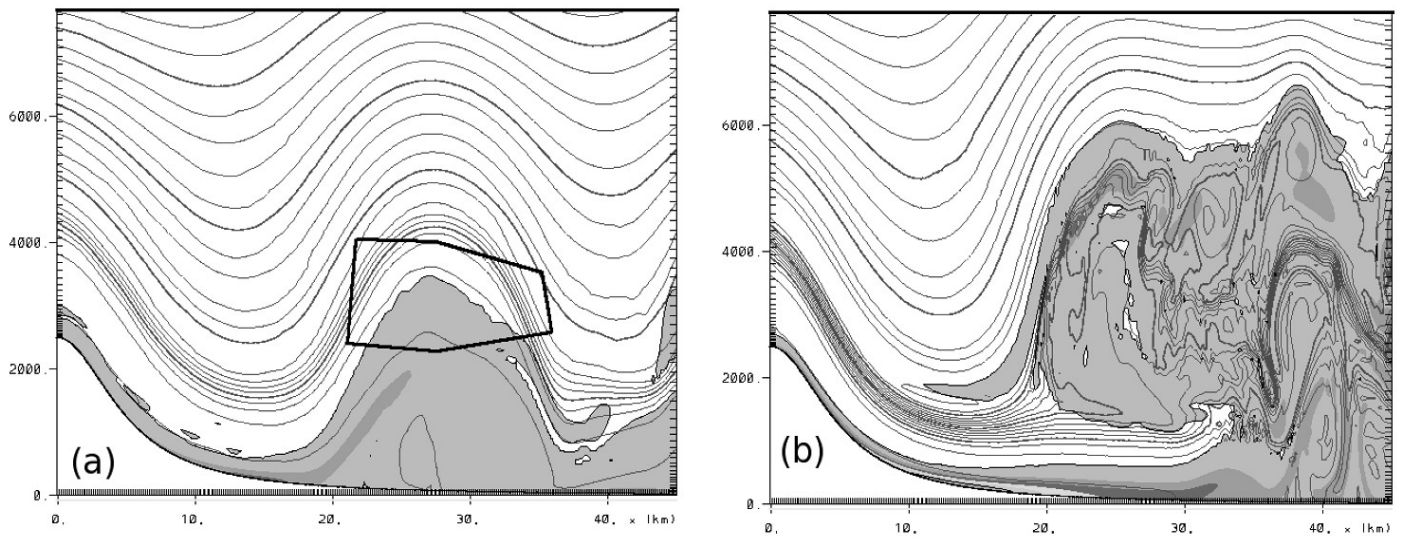


Figure 1 Results from simulations of two rotor types.³ Potential temperature is contoured (1 K interval), while shading indicates turbulent regions. (a) Type-1 wave/rotor. Box shows typical flight path – flown in a clockwise direction – through Type-1 rotors during research flights. (b) Type-2 wave/rotor. Note the higher-reaching, more widespread turbulence associated with the Type-2 rotor.

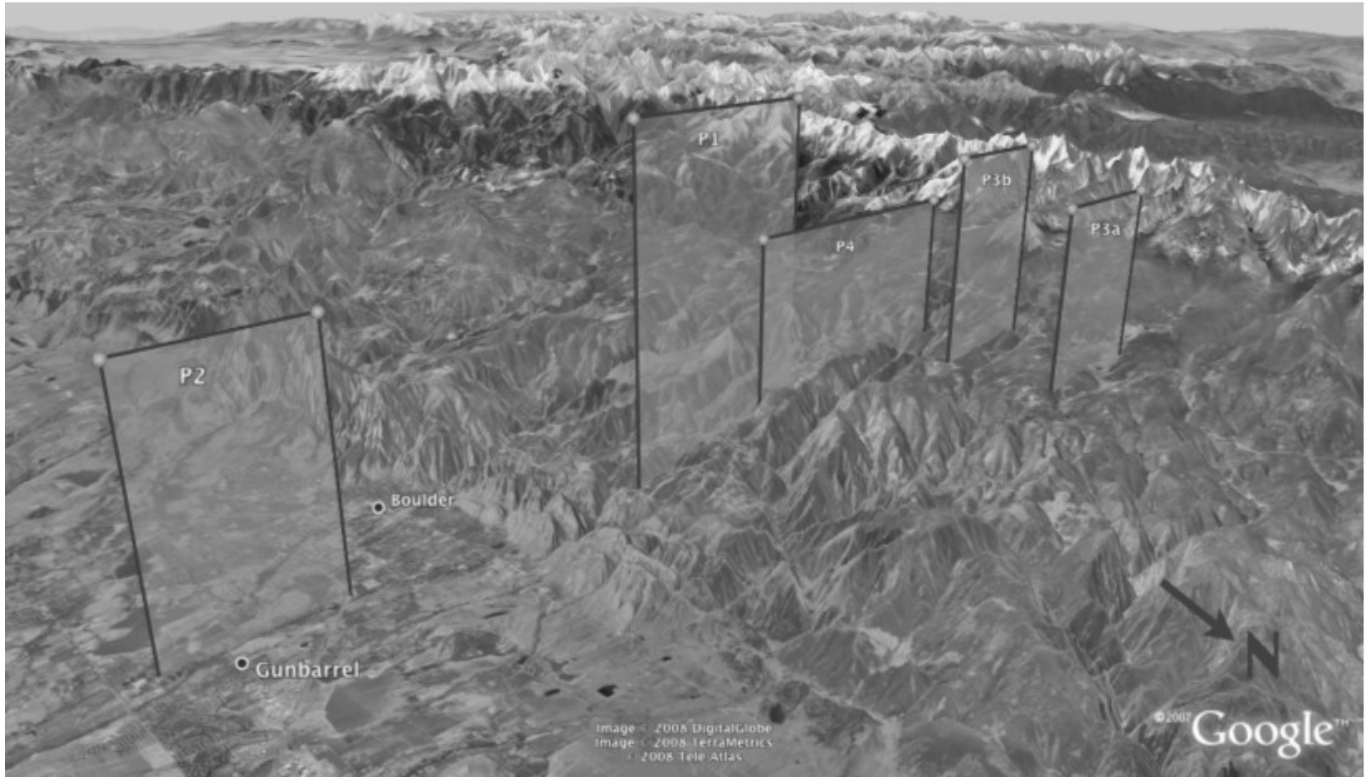


Figure 2 Topography along the Front Range of the Colorado Rocky Mountains. Flights originated just east of the point marked 'Boulder'. Approximate locations and heights of the rotor penetrations are indicated by the rectangles. (Image produced using Google Earth mapping service).

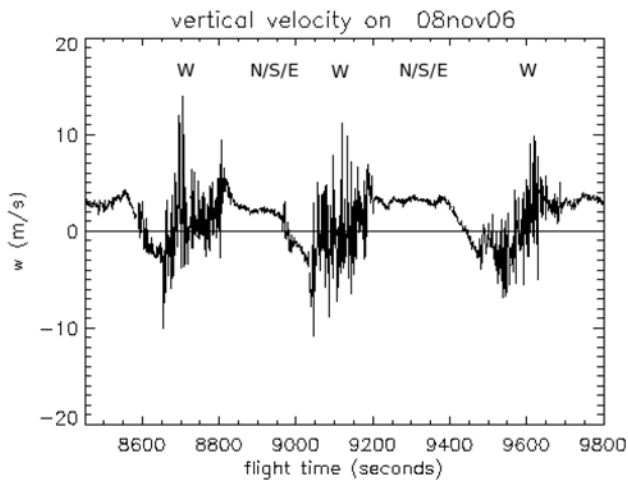


Figure 3 Time series of vertical velocity derived from the DDV for three (of six) rotor penetrations flown on 08 Nov 06. The time series represents successive penetrations flown in one location. Approximate sailplane heading is indicated above the time series. Rotor penetrations were flown from east to west (in an upwind direction).

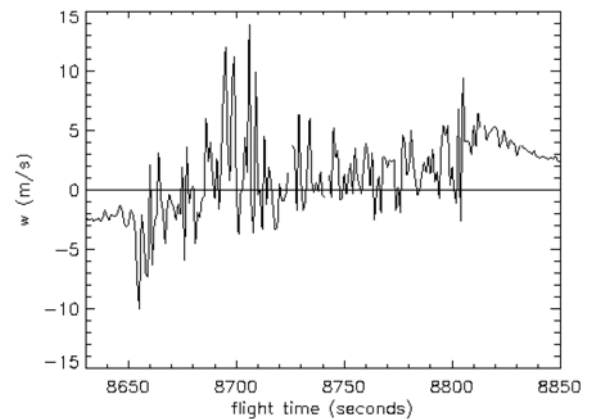


Figure 4 Vertical velocity time series for the first rotor penetration in Fig. 3, showing details of small-scale eddies embedded within the parent rotor.

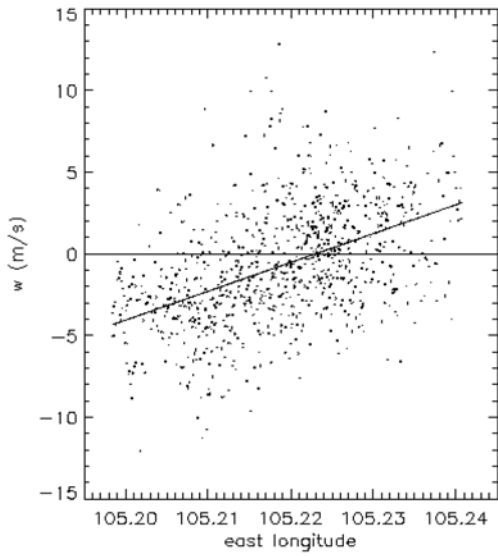


Figure 5 Scatter plot of all six rotor penetrations flown on 08 November 2006. Each point represents one vertical velocity measurement and its longitude. The zero vertical velocity line is drawn as well as a linear fit to the data.

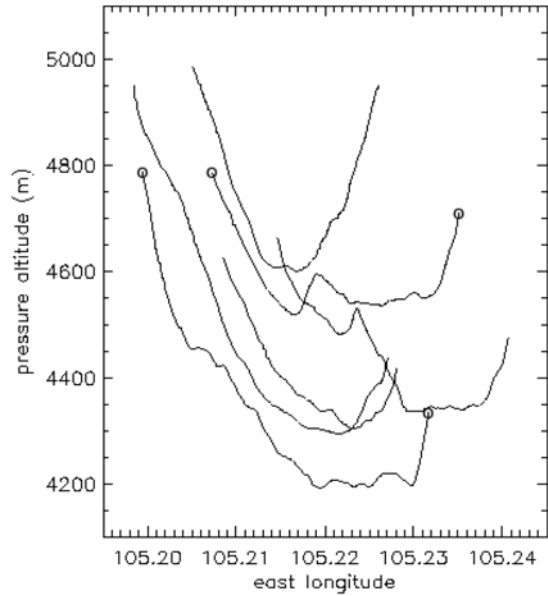


Figure 6 Flight tracks from all six rotor penetrations flown on 08 November 2006. The circles at the ends of two tracks are discussed in the text.

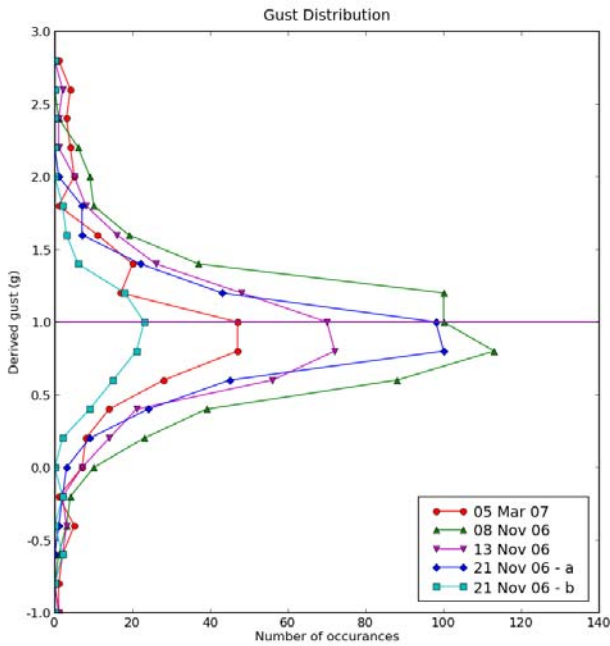


Figure 7 Distribution of gusts derived from vertical velocity for each of the four dates shown in Table 1 on which data was successfully collected.